PAPER

Conformational properties of alkyl glucosyl sulfones in solution†

Carlos A. Sanhueza, [ID] [a,b] Rosa L. Dorta [ID] [a] and Jesús T. Vázquez [ID] *[a]

The conformational properties of ester-protected alkyl glucosyl sulfones were studied by means of nuclear magnetic resonance (NMR) and circular dichroism (CD). The equilibrium about the C5−C6 rotational axis (hydroxymethyl group) in polar and apolar media is distributed between the *gg* and *gt* rotamers, and the equilibrium contributions of each rotamer are modulated by the steric properties of the aglycone, where an increment in the alkyl substituent's bulkiness leads to progressive increments in *gt* contributions at the expense of *gg*. The equilibrium about the glycosidic bond is also dependent on the aglycone's bulkiness and appears more sensitive to the media polarity. Glucosyl sulfones carrying small aglycones, *e.g*, those substituted with methyl and ethyl groups, show a ϕ torsion predominated by the *g+* conformer in apolar media (C_6D_6) and distributed between *g−* and *g+* conformers in a polar solvent (CD_3CN). Compounds substituted with larger alkyl groups, such as iso-propyl and *tert*-butyl groups, show glycosidic bond conformations predominated by the *g−* conformer.

Introduction

Carbohydrates are intrinsically flexible molecules playing critical roles in living systems.[1] The molecular recognition of cell-associated saccharides by protein receptors typically triggers a plethora of physiological and pathological functions including fertilization,[2] immunity,[3] infection,[4] metastasis,[5] and many others.[6] To successfully elicit such functions, the carbohydrate ligand must fulfill geometrical and conformational requirements for an optimal interaction with the receptor. Hence, the study of the conformational properties of carbohydrates is vital to fully characterize and understand the molecular recognition mechanisms at the molecular level. Moreover, understanding the conformational patterns of sugars and the factors driving them could prove useful in future studies of carbohydrates and glycomimetics.

The conformational flexibility of hexopyranoses, the prevalent monosaccharide configuration in mammalian glycans, lies on the glycosidic C1–O1 bond and the C5–C6 bond (hydro-

*[a]Departamento de Química Orgánica, Instituto Universitario de Bio-Orgánica
"Antonio González", Universidad de La Laguna, Avda. Astrofísico Francisco Sánchez
2, La Laguna, Tenerife 38206, Spain. E-mail: jtruvaz@ull.edu.es*
*[b]Department of Pharmaceutical Sciences, St John's University, 8000 Utopia Parkway,
Queens, NY 10439, USA*

†Electronic supplementary information (ESI) available: ^{1}H and ^{13}C NMR spectra of all alkyl glucosyl sulfones, including expansions of their H5 and H6 signals; some selected 1D NOESY experiments; tables with experimental and calculated NMR data; overlaid regions of experimental and simulated ^{1}H NMR spectra, as well as plots of calculated rotamer populations from simulated spectra *vs.* Charton parameters. See DOI: https://doi.org/10.1039/d4ob02056a

xymethyl group) (Fig. 1A). The torsional angles ϕ and ψ characterize the glycosidic bond's conformation. The free rotation about ϕ generates three staggered rotamers called *exo–syn* (or *g−*), *exo–anti* (or *g+*), and *non-exo* (or *anti*) (Fig. 1B) whose contributions to the glycosidic conformational equilibrium are determined by the regio- and stereochemistry of the glycosidic
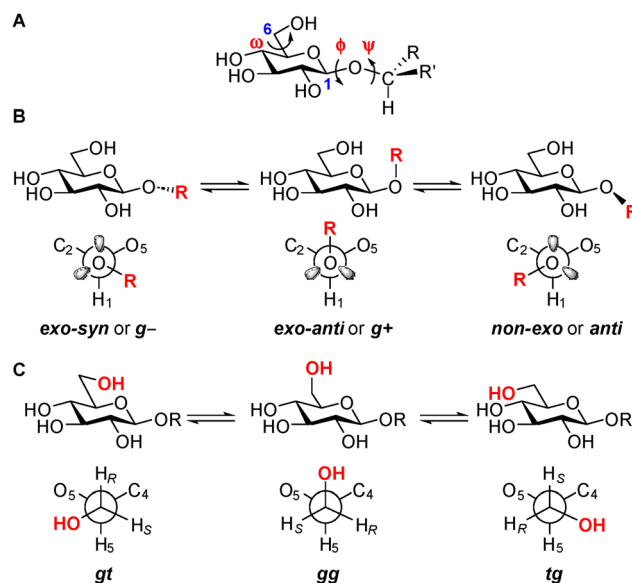

Fig. 1 Conformational properties of glycosides. (A) Flexible bonds in *O*-glycosides; (B) glycosidic bond rotamers; (C) hydroxymethyl group rotamers.
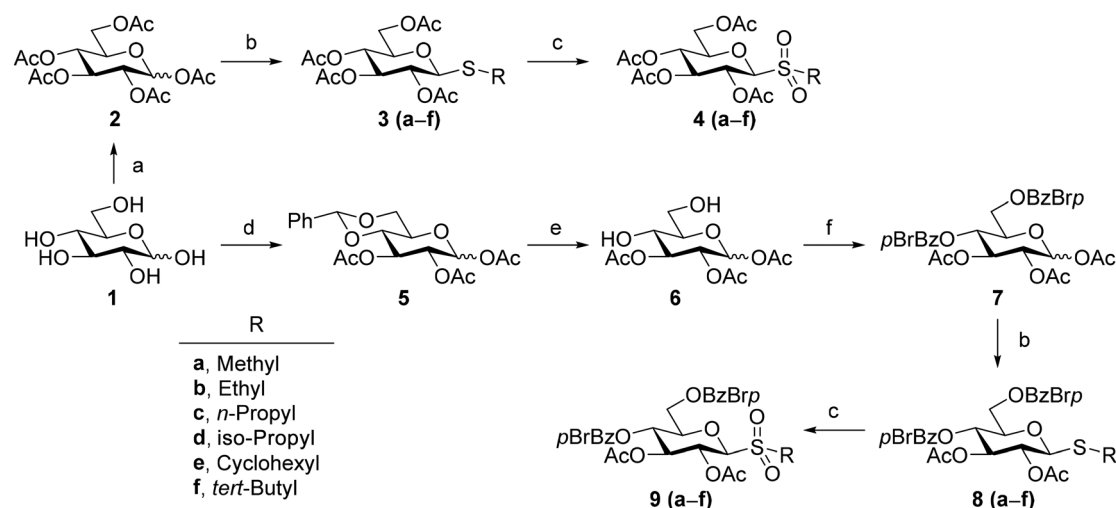
linkage, the media polarity, the anomeric effect, and the presence of intramolecular polar interactions. For example, in aryl S-β-glucosides, the aglycone's electronic properties appear to be a relevant conformational modulator about ϕ, where *exo–syn* is the predominant conformer in glucosides carrying electron-deficient aryl rings whereas those carrying electron-richer substituents exhibit larger *exo–anti* and *non–exo* contributions.[7] The free rotation about ω (hydroxymethyl group) generates three rotamers called *gauche–gauche* (*gg*), *gauche–trans* (*gt*), and *trans–gauche* (*tg*) (Fig. 1C). The contributions of each rotamer to the conformational equilibrium about C5–C6 depend on several factors including the stereochemical configuration of C4, the nature of the C4 and C6 substituents, the polarity of the media, the anomeric configuration, and the chemical nature of the aglycone, including its stereochemistry. We have extensively studied the effect of the aglycone's nature on the hydroxymethyl conformation of alkyl O-,[8] S-,[9] and C-[10] glycosides as well as glycosyl sulfoxides,[11] finding that the rotameric distribution about C5–C6 relates to the steric properties of the alkyl aglycone, where a progressive increment of its bulkiness leads to a correlating increment of *gt* percent contributions at the expense of the predominant *gg* conformer. We found a similar conformational behavior in aryl S-glycosides, where increased *gt* contributions correlate with glycosides carrying stronger electron-withdrawing aryl substituents.[7] The elimination of the endocyclic oxygen atom leads to carbasugar derivatives showing no conformational dependence on the aglycone's nature.[12] We envisage these structure–conformation relationships as an invaluable tool for upcoming studies of conformationally modulated carbohydrates and glycomimetics that could be useful in areas such as drug discovery and molecular probe design. In our pursuit to expand our knowledge on structure–conformation relationships, we centered our attention on the glycosidic and hydroxymethyl flexibility of alkyl glucosyl sulfones. Glycosyl sulfones are an underexplored, yet promising, class of glycosyl donors capable of generating cationic and radical glycosylating intermediates.

Synthesis and structural characterization of alkyl glycosyl sulfones

We designed two series of model compounds namely acetates (**4a–4f**) and dibenzoates (**9a–9f**) suitable for performing the conformational analysis by nuclear magnetic resonance (NMR) and circular dichroism (CD) respectively (Scheme 1). We started the preparation of acetates **4a–4f** from free glucose **1**, which was converted into glucose *per*-acetylated by treatment with Ac_2O in pyridine at room temperature. The anomeric acetate in **2** was then substituted by an alkyl thiyl group by treating the glycosyl donor with $BF_3\cdot Et_2O$ in DCM in the presence of the respective alkyl thiol.[13] This procedure afforded alkyl S-glycosides **3b–3f** in moderate to good yields.[9] Since the volatility of methanethiol makes its direct glycosylation difficult to implement, methyl derivative **4a** was prepared by the *in situ* methylation of a glucosyl thiouronium salt prepared by refluxing a MeCN solution of **2**, thiourea, and $BF_3\cdot Et_2O$.[9,14] The subsequent oxidation of S-glycosides **3a–3f** with *per*-acetic acid, generated *in situ* by reacting H_2O_2 with Ac_2O over SiO_2 as a catalyst,[15] afforded the respective alkyl glycosyl sulfones **4a–4f** in excellent yields (91–99%). To prepare dibenzoates **9a–9f**, we subjected the C4 and C6 hydroxyl groups in **1** to regioselective protection as benzylidene acetal by treatment with benzaldehyde dimethoxy acetal and *p*-toluenesulphonic acid in DMF at 50 °C. The resulting benzylidene was subsequently *per*-acetylated with Ac_2O in pyridine to afford **5** as an anomeric mixture. The C4/C6 diol **6** was obtained by dissolving **5** in an $AcOH/H_2O$ (4 : 1) mixture and heating at 60 °C. Subsequent installation of the *p*-bromobenzoate chromophores over C4 and C6, required for CD analysis, was accomplished by react-

Scheme 1 Synthesis of alkyl glucosyl sulfones. Conditions: (a) Ac_2O, pyridine, rt; (b) for **4b–4f** and **8b–8f**: R–SH, $BF_3\cdot OEt_2$, DCM, rt 4–12 h; for **4a** and **8a**: (i) $(NH_2)_2CS$, $BF_3\cdot OEt_2$, MeCN, reflux; (ii) Et_3N, CH_3I, reflux; (c) H_2O_2, Ac_2O, silica gel 60, DCM, rt; (d) (i) $PhCH(OMe)_2$, *p*-TsOH, DMF, 50 °C; (ii) Ac_2O, pyridine, rt; (e) $AcOH/H_2O$ (8 : 2), 60 °C; (f) *p*-BrBzCl, pyridine, DMAP, 60 °C.

R
a, Methyl
b, Ethyl
c, *n*-Propyl
d, iso-Propyl
e, Cyclohexyl
f, *tert*-Butyl

This journal is © The Royal Society of Chemistry 2025

Org. Biomol. Chem., 2025, **23**, 7000–7012 | **7001**

ing **6** with *p*-bromobenzoyl chloride and DMAP in pyridine at 60 °C. The resulting glycosyl donor **7** was dissolved in DCM and activated with $BF_3 \cdot Et_2O$ in the presence of different alkyl thiols to afford the respective *S*-glycosides **8b–8f** in good yields (40–55%).[9] Methyl *S*-glycoside **8a** was prepared in 42% yield *via* methylation of the respective glucosyl thiouronium salt.[9] The oxidation of alkyl *S*-glycosides **8a–8f** with H_2O_2 in the presence of Ac_2O and silica gel in DCM afforded the target alkyl glycosyl sulfones **9a–9f** in excellent yields (92–98%).
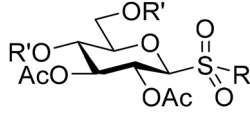
The characterization of the glycosyl sulfones was performed by means of 1D (^1H, $^{13}C\{^1H\}$, 1D-NOESY) and 2D (COSY, HSQC) NMR spectroscopy. The β anomeric configuration was determined from the $^3J_{H1,H2}$ coupling constants which oscillated between 9.4 to 9.9 Hz among sulfones from both series. Moreover, the assigned anomeric stereochemistry was confirmed from the observed cross-peaks between the anomeric proton H1 with H3 and H5 in the selective 1D-NOESY experiments.

Results and discussion

The correct identification of the pro-chiral H6*S* and H6*R* protons is critical for the correct assessment of the conformational equilibrium about ω. We identified H6*S* and H6*R* following the protocol established by Ohrui *et al.*[16] Briefly, in ester-protected D-glucopyranosides, H6*R* appears downfield with respect to H6*S* (δH6*R* > δH6*S*) and the $^3J_{H5,H6R}$ coupling constant values are higher than $^3J_{H5,H6S}$ regardless of the protective group patterns and media. All synthesized glycosyl sulfones showed well-isolated H6*R* and H6*S* peaks in their ^1H NMR spectra, and the reported δH6*R* > δH6*S* relationship is fulfilled by the *per*-acetates **4a** (R = Me), **4b** (R = Et) and **4c** (R = *n*-Pr). As the size of the alkyl aglycones increases, we observe progressive H6*R* deshielding and H6*S* shielding, resulting in sulfones **4d** (R = i-Pr), **4e** (R = Cy), and **4f** (R = *t*-Bu) showing H6*S* downfield with respect to H6*R* (δH6*S* > δH6*R*). In the dibenzoate series, H6*S* appears downfield with respect to H6*R* in all derivatives. Because of this discrepancy, which probably originated from a combination of the anisotropic effect of the sulfinyl group and the conformational preferences about ϕ and ω, we assigned the proton identities based on the $^3J_{H5,H6R}$ and $^3J_{H5,H6S}$ values. Since in simple glucosides, the contributions of the *tg* rotamer to the C5–C6 conformational equilibrium are negligible, we expect low $^3J_{H5,H6S}$ and high $^3J_{H5,H6R}$ values, reflecting the predominance of the *gg* and *gt* rotamers typically observed on glucosides.

Table 1 collects selected NMR data (CDCl₃) for acetates **4a–4f** and dibenzoates **9a–9f**. In the acetates, we can observe an interesting trend in the chemical shifts of H6*R* and H6*S* with respect to the aglycone's structure. As the alkyl substituent's bulkiness increases, δH6*R* moves upfield whereas δH6*S* moves downfield. Thus, H6*R* progressively shields from 4.32 (**4a**, R = Me) to 4.13 ppm (**4f**, R = *t*-Bu) and H6*S* deshields from 4.20 (**4a**, R = Me) to 4.24 ppm (**4f**, R = *t*-Bu), with H6*R* being the proton exhibiting the largest Δδ of 0.19 ppm (*vs.* Δδ =

Table 1 Selected ^1H and $^{13}C\{^1H\}$ NMR data (CDCl₃) for alkyl glucosyl sulfones **4a–4f** and **9a–9f**

Cmpd	R	δC1	δH1	δH6*R*	δH6*S*
Acetate series (R′ = Ac)					
4a	Me	88.4	4.35	4.32	4.20
4b	Et	87.5	4.46	4.26	4.21
4c	*n*-Pr	87.8	4.42	4.26	4.20
4d	i-Pr	85.9	4.63	4.20	4.23
4e	Cy	85.7	4.60	4.16	4.22
4f	*t*-Bu	86.3	4.84	4.13	4.24
Dibenzoate series (R′ = *p*-BrBz)					
9a	Me	88.2	4.47	4.44	4.62
9b	Et	87.4	4.58	4.44	4.60
9c	*n*-Pr	87.8	4.54	4.44	4.60
9d	i-Pr	85.8	4.74	4.43	4.56
9e	Cy	85.6	4.70	4.42	4.55
9f	*t*-Bu	86.4	4.95	4.39	4.57

0.04 ppm for H6*S*). In contrast, both δH6*R* and δH6*S* in dibenzoates **9a–9f** show a small upfield displacement (Δδ = 0.05 ppm) as the aglycone becomes bulkier. The chemical shifts of the anomeric proton (H1) and carbon (C1) also appear to depend on the aglycone's structure in both sulfone series, where δH1 moves downfield and δC1 upfield as the aglycone increases its volume. In the acetate series, the anomeric proton H1 deshields from 4.35 (**4a**, R = Me) to 4.84 ppm (**4f**, R = *t*-Bu) (Δδ = 0.49 ppm) and from 4.47 (**9a**, R = Me) to 4.95 ppm (**9f**, R = *t*-Bu) in the dibenzoates (Δδ = 0.48 ppm). In turn, the anomeric carbon shields from 88.4 (**4a**, R = Me) to 86.3 ppm (**4f**, R = *t*-Bu) in the acetates (Δδ = 2.1 ppm) and from 88.2 (**9a**, R = Me) to 86.4 ppm (**9f**, R = *t*-Bu) in the dibenzoates (Δδ = 1.8 ppm).

Conformational analysis of the hydroxymethyl group

We analyzed the acetates **4a–4f** and dibenzoates **9a–9f** in media with different polarities. The observed $^3J_{H5,H6R}$ and $^3J_{H5,H6S}$ values in each solvent are collected in Table 2 for acetates **4a–4f** and in Table 3 for dibenzoates **9a–9f**. In the acetate series, analyzed in CDCl₃, we observe $^3J_{H5,H6R}$ values to vary between 4.7 and 6.5 Hz whereas $^3J_{H5,H6S}$ shows smaller fluctuations between 2.1 and 2.4 Hz. Moreover, we observe a $^3J_{H5,H6R}$ dependency on the aglycone's structure, namely $^3J_{H5,H6R}$ increases as the aglycone becomes bulkier. Thus, glycosides **4a** (R = Me), **4b** (R = Et), **4c** (R = *n*-Pr) and **4d** (R = i-Pr) show $^3J_{H5,H6R}$ values of ~4.8 Hz which increase to 5.6 and 6.5 Hz in cyclohexyl (**4e**) and *tert*-butyl (**4f**) derivatives respectively. We observe the same trend for the dibenzoates in CDCl₃. In this series, methyl derivative **9a** shows a $^3J_{H5,H6R}$ value of 4.9 Hz which progressively increases to 6.7 Hz in *tert*-butyl sulfone **9f**. The $^3J_{H5,H6S}$ values range from 2.1 to 2.4 Hz for this series in CDCl₃. The analysis of the $^3J_{H5,H6R}$ and $^3J_{H5,H6S}$ data in the remaining solvents shows the same trends for both sulfone series. Regardless of the solvent's polarity, $^3J_{H5,H6R}$ exhibits

7002 | *Org. Biomol. Chem.*, 2025, **23**, 7000–7012

This journal is © The Royal Society of Chemistry 2025

Table 2 $^3J_{H5,H6R}$ and $^3J_{H5,H6R}$ coupling constants in various solvents for alkyl glucosyl sulfones **4a–4f**

Cmpd	R	C_6D_6		$CDCl_3$		CD_3OD		CD_3CN	
		$^3J_{H5,H6R}$	$^3J_{H5,H6S}$	$^3J_{H5,H6R}$	$^3J_{H5,H6S}$	$^3J_{H5,H6R}$	$^3J_{H5,H6S}$	$^3J_{H5,H6R}$	$^3J_{H5,H6S}$
4a	Me	4.7	2.0	4.8	2.2	4.9	2.3	5.1	2.4
4b	Et	4.8	2.2	4.7	2.1	5.0	2.2	5.4	2.4
4c	n-Pr	4.8	1.9	4.8	2.3	5.0	2.3	5.4	2.4
4d	i-Pr	4.4	3.0	4.8	2.4	5.4	2.4	6.0	2.4
4e	Cy	5.4	2.2	5.6	2.3	5.4	2.4	5.3	3.0
4f	t-Bu	6.4	2.2	6.5	2.4	6.2	2.4	6.1	2.9

Table 3 $^3J_{H5,H6R}$ and $^3J_{H5,H6S}$ values for alkyl glucosyl sulfones **9a–9f** in $CDCl_3$ and CD_3CN

Cmpd	R	$CDCl_3$		CD_3CN	
		$^3J_{H5,H6R}$	$^3J_{H5,H6S}$	$^3J_{H5,H6R}$	$^3J_{H5,H6S}$
9a	Me	4.9	3.0	4.7	3.0
9b	Et	5.3	3.0	5.0	3.0
9c	n-Pr	5.4	3.0	5.1	3.0
9d	i-Pr	5.8	2.7	5.5	2.9
9e	Cy	5.9	2.4	5.7	2.8
9f	t-Bu	6.7	2.3	6.3	2.1

larger values that increase as the aglycone's size increases whereas $^3J_{H5,H6S}$ shows smaller values with small fluctuations throughout each series.

Due to the small chemical shift differences between H6R and H6S in the ^{1}H NMR spectra, ABX systems were obtained. To test how this could affect the values of $^3J_{H5,H6R}$ and $^3J_{H5,H6S}$, we proceed to simulate the NMR regions containing H6R, H6S, H5 and H4 as an ABXY pattern for acetylated sulfones **4a–4f** ($CDCl_3$ and CD_3CN) and dibenzoates **9a–9f** ($CDCl_3$) using the built-in algorithm (DAISY) in Bruker TopSpin 4.0.7. The overlaid spectral comparison between those obtained directly and those after simulation is in excellent agreement, either in chemical shifts or in coupling constants (ESI Tables S2–S4 and Fig. S26–S45†). Both analyses show the same general behaviour, an increase and a decrease in the $^3J_{H5,H6R}$ and $^3J_{H5,H6S}$ values, respectively, as the bulkiness of the alkyl group increases. The conformational information contained in the $^3J_{H5,H6R}$ and $^3J_{H5,H6S}$ constants was converted into percent contributions of gg, gt, and tg (P_{gg}, P_{gt}, and P_{tg}) using eqn (1)–(3), developed by Crich et al.[17] These equations include optimized

limiting coupling constants for the gg, gt, and tg rotamers allowing for accurate P_{gg}, P_{gt}, and P_{tg} calculations.

$$^3J_{H5,H6R} = 1.0\ P_{gg} + 11.0\ P_{gt} + 4.8\ P_{tg} \quad (1)$$

$$^3J_{H5,H6S} = 2.2\ P_{gg} + 2.5\ P_{gt} + 10.2\ P_{tg} \quad (2)$$

$$1 = P_{gg} + P_{gt} + P_{tg} \quad (3)$$

Table 4 shows the calculated gg, gt, and tg rotamer populations for the acetyl derivatives **4a–4f** and Table 5 presents the respective conformational data for dibenzoates **9a–9f** obtained by using the experimental data contained in Tables 2–3.

In the per-acetylated glucosyl sulfones **4a–4f**, the conformational equilibrium about ω distributes between the gg and gt rotamers with small to no contributions of tg in all solvents. Independent of the media polarity, the gg conformer predominates the equilibrium in most sulfones. However, the gg predominance clearly depends on the aglycone's nature since P_{gg} progressively declines as the size of the alkyl substituent increases, and this P_{gg} detriment correlates with a progressive

Table 5   Calculated gg, gt and tg rotational populations in $CDCl_3$ and CD_3CN for sulfones **9a–9f**

Cmpd	R	$CDCl_3$			CD_3CN		
		P_{gg}	P_{gt}	P_{tg}	P_{gg}	P_{gt}	P_{tg}
9a	Me	56	36	8	58	34	8
9b	Et	52	40	8	55	37	8
9c	n-Pr	51	41	8	54	38	8
9d	i-Pr	49	46	5	51	42	7
9e	Cy	51	49	0	49	45	6
9f	t-Bu	44	46	0	48	52	0

Table 4   Calculated gg, gt, and tg rotational populations for sulfones **4a–4f** in various solvents

Cmpd	R	C_6D_6			$CDCl_3$			CD_3OD			CD_3CN		
		P_{gg}	P_{gt}	P_{tg}	P_{gg}	P_{gt}	P_{tg}	P_{gg}	P_{gt}	P_{tg}	P_{gg}	P_{gt}	P_{tg}
4a	Me	63	37	0	62	38	0	61	39	0	58	41	1
4b	Et	62	38	0	63	37	0	60	40	0	56	44	0
4c	n-Pr	62	38	0	62	38	0	60	40	0	56	44	0
4d	i-Pr	61	31	8	61	38	1	56	44	0	50	50	0
4e	Cy	56	44	0	54	46	0	56	44	0	52	40	8
4f	t-Bu	46	54	0	45	55	0	48	52	0	45	48	7

increment in the *gt* contributions. In C_6D_6, the lowest polarity solvent used in this study, *gg* shows a 63% contribution in the methyl-substituted compound **4a**, which falls to 46% in the *tert*-butyl sulfone **4f**, whereas the *gt* contribution correspondingly increases from 37% (**4a**, R = Me) to 54% (**4f**, R = *t*-Bu). Similarly, in CDCl₃, P_{gg} diminishes from 62% (**4a**, R = Me) to 45% (**4f**, R = *t*-Bu) and P_{gt} increases from 38% (**4a**) to 55% (**4f**). In CD₃OD, the population fluctuations are P_{gg}: 61% (**4a**)/48% (**4f**) and P_{gt}: 39% (**4a**)/52% (**4f**) and in CD₃CN, they are P_{gg}: 58% (**4a**)/45% (**4f**) and P_{gt} 41% (**4a**)/48% (**4f**).

Regarding the *tg* rotamer, three *per*-acetylated sulfones exhibit *tg* contributions with the iso-propyl derivative **4d** being the only compound showing *tg* contributions in two different media with P_{tg} values of 8% and 1% in C_6D_6 and CDCl₃, respectively. In CD₃CN, methyl, cyclohexyl and *tert*-butyl sulfones **4a**, **4e** and **4f** show small 1%, 8%, and 7% *tg* contributions, respectively.

The C5–C6 conformational dependency on the aglycone's substituent is also present in the dibenzoates. For compounds **9a–9f** we observe an equilibrium predominated by *gg* and *gt* regardless of the media polarity. In CDCl₃, methyl sulfone **9a** shows a *gg* contribution of 56% which progressively diminishes to 44% in the *tert*-butyl derivative **9f**, while the *gt* population increases from 36% (**9a**, R = Me) to 46% (**9f**, R = *t*-Bu). Likewise, in CD₃CN, the *gg* population gradually decreases from 58% (**9a**, R = Me) to 48% (**9f**, R = *t*-Bu) and correspondingly, the *gt* population increases from 34% (**9a**) to 52% (**9f**). In both CDCl₃ and CD₃CN, the *tg* contributions remain about ~8% for most sulfones. Dibenzoates show larger *tg* contributions compared with their parent acetates, probably by a favorable π–π interaction between the two aromatic rings, and independently of the media, the *tg* rotamer decreases its population from the methyl (**9a**, 8%) to the *tert*-butyl (**9f**, 0%) derivative, favoring the *gt* population.

Given the evident relationship between the hydroxymethyl's rotational populations and the aglycone's volume, we represented the calculated P_{gg} and P_{gt} data set *versus* the Charton values (ν) of the respective alkyl substituents Fig. 2.[24] The Charton value is a steric descriptor derived from Taft's steric parameter[24,25a–d] which was developed to include electronic factors and is a practical choice for a broader understanding of steric trends across physicochemical phenomena.[26] From the P_{gg} and P_{gt} *versus* ν plots shown in Fig. 2, the linear relationship between the rotational populations and the steric descriptor becomes clear. In both *per*-acetyl and dibenzoate series, we observe a positive linear correlation of *gt* with ν and a negative one for *gg* in all analysed solvents. As the Charton value increases, *i.e.*, the aglycone's alkyl substituent becomes bulkier, the *gt* population linearly increases at the expense of *gg* until reaching predominance in sulfones **4f** and **9f**, both substituted with the bulkiest alkyl group examined in this study.

This relationship between aglycone's bulkiness and rotational populations was also observed in the respective P% *vs.* ν plots performed based on the calculated $^3J_{H5,H6R}$ and $^3J_{H5,H6S}$ values (algorithm DAISY, in Bruker TopSpin 4.0.7.),

confirming the above-mentioned conclusion (see ESI Table S5 and Fig. S46–S48†).

Study of hydroxymethyl conformation by circular dichroism

Circular dichroism (CD) is a powerful technique that has been mainly used for the determination of absolute configurations of a great number of compounds of both natural and synthetic origin. Further developments came with the CD exciton chirality method,[27] which allows the determination of absolute configurations in a non-empirical way. Applications of circular dichroism have also been widely applied to the conformational studies in a solution of small-to-medium sized molecules, as well as macromolecules, especially proteins.[28]

The CD exciton chirality method is based on the through-space interaction of the electric transition moments of two chromophores that gives rise to an excited state split into two energy levels. Excitations to these levels lead to a CD spectrum with two Cotton effects of opposite signs, namely to a "split" CD curve. The chiral environment of the two chromophores determines the sign of the Cotton effects, with the sign of the exciton chirality being that of the first Cotton effect, the one at a longer wavelength (Fig. 3).

In the belief that CD is an extremely sensitive spectroscopic technique to study the rotational population of the hydroxymethyl group in alkyl glucopyranoside sulfones, the CD spectra of compounds **9a–9f** were recorded in CH₃CN.

The CD curves of compounds **9a–9f** (Fig. 4) showed a first Cotton effect around 251 nm and a second Cotton effect around 233 nm, centered around the UV λ_{max} 245 nm (Table 6), in agreement with the exciton chirality method. In addition, a general decrease in the intensities of the first and second Cotton effects, or their *A* values, from the methyl derivative **9a** (*A* value 21.5), to the ethyl derivative **9b** (19.4), to the *n*-propyl **9c** (18.7), to the isopropyl **9d** (16.3), to the cyclohexyl **9e** (14.2), and to the *tert*-butyl derivative **9f** (11.2), can be observed.

According to the sign of the pairwise interaction between the chromophores at the 4 and 6 positions in the *gg*, *gt* and *tg* rotamers (Fig. 5), the general decrease in the CD Cotton effects can only be explained by a decrease in the population of the *gg* rotamer (positive contribution) and an increase in the population of the *gt* rotamer (negative contribution).

CD and ¹H NMR data comparison indicated the existence of an excellent correlation between the magnitudes of the rotamer populations obtained by ¹H NMR and the CD *A* values.

Conformational analysis of the glycosidic bond

To gain a deeper insight into the flexibility of alkyl glucosyl sulfones, we examined the conformational properties about the ϕ (H1–C1–S–C) torsion angle by means of selective 1D-NOESY spectroscopy. The free rotation about C1–S, either for glucosyl sulfoxides or sulfones, generates three staggered rotamers called *g*−, *g*+ and *anti* (Fig. 6), based on the spatial relationship between the aglycone's carbon directly attached to the sulfur atom and the endocyclic oxygen O5.
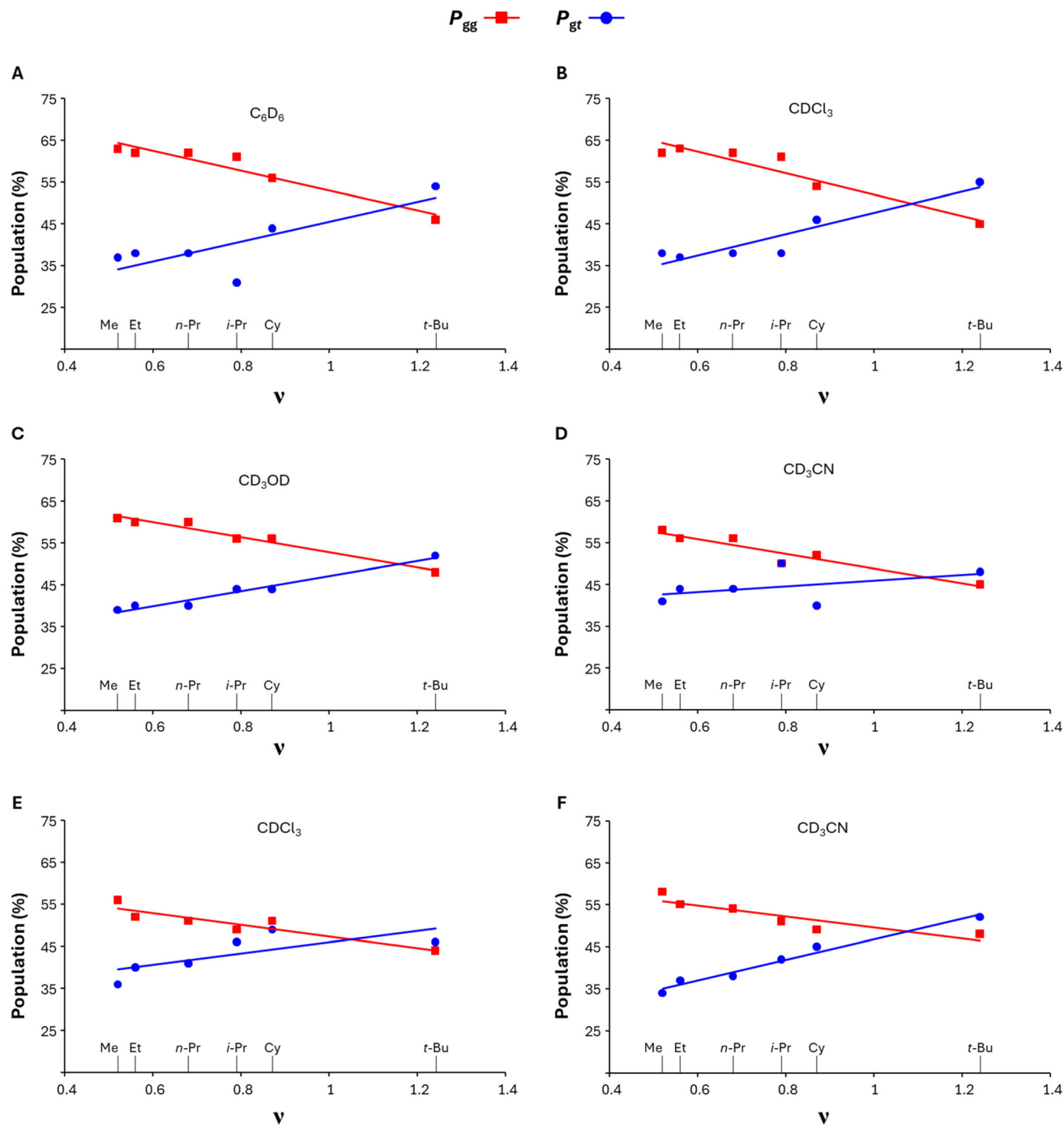
7004 | *Org. Biomol. Chem.*, 2025, **23**, 7000–7012

This journal is © The Royal Society of Chemistry 2025

Fig. 2 P_{gg} (red color) and P_{gt} (blue color) *versus* alkyl's Charton values (ν) for *per*-acetylated glucosyl sulfones **4a–4f** in: (A) C_6D_6;[18] (B) $CDCl_3$;[19] (C) CD_3OD;[20] (D) CD_3CN;[21] and for dibenzoate glucosyl sulfones **9a–9f** in: (E) $CDCl_3$;[22] (F) CD_3CN.[23]

As can be observed in Fig. 7, for the *g*– conformer, we anticipate nOe couplings between H1 and the aglycone's protons closer to the sulfur, whereas for the *g*+ conformer, we expect similar nOe couplings between the aglycone's protons and H2. In C2-substituted β-glucosides, the *anti* rotamer is heavily destabilized by steric repulsions and we do not expect significant contributions from it. Therefore, we carried out selective 1D-NOESY experiments in C_6D_6 (apolar) and CD_3CN

(polar) for the *per*-acetylated sulfones **4a** (R = Me), **4b** (R = Et), **4d** (R = i-Pr), and **4f** (R = t-Bu), thus representing glucosides carrying methyl, primary, secondary, and tertiary alkyl aglycones.

Fig. 8 shows stacked sections of the 1D-NOESY spectra for selected sulfones. We selectively excited the alkyl's hydrogen atoms closer to H1 and H2 corresponding to the methyl group in **4a**, the ethyl's methylene in **4b**, the iso-propyl's methine in
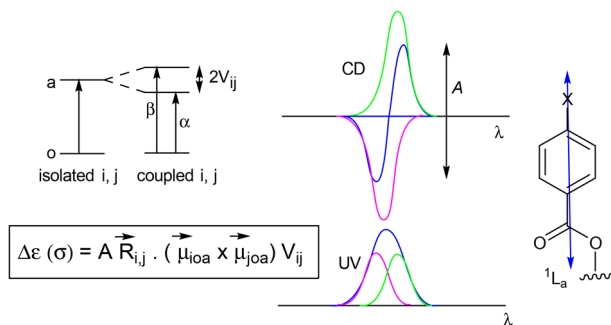
This journal is © The Royal Society of Chemistry 2025

Org. Biomol. Chem., 2025, **23**, 7000–7012 | **7005**

Fig. 3 Nondegenerate system in which chromophoric groups *i* and *j* undergo O → a transitions to give split levels separated by interaction energy $2V_{ij}$. $\Delta\varepsilon$ is the molar circular dichroism, $R_{i,j}$ is the interchromophoric distance vector from *i* to *j*, and μ_{ioa} and μ_{joa} are electric transition dipole moments of excitation O → a. ^1L_a is the transition dipole moment in *p*-substituted benzoate chromophores.
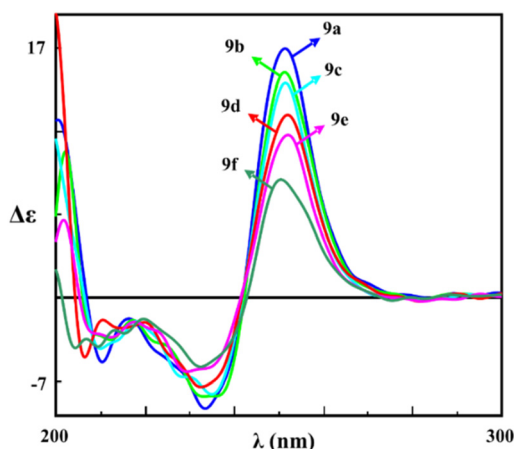

Fig. 4 CD curves (CH$_3$CN) for alkyl glucosyl sulfones **9a−9f** at 25 °C.

Table 6 Wavelength, intensity of the Cotton effects and *A* values of the CD spectra for sulfones **9a−9f** (CH$_3$CN)

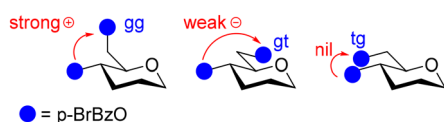| Cmpd	R	First Cotton effect		Second Cotton effect		
		λ (nm)	$\Delta\varepsilon$	λ (nm)	$\Delta\varepsilon$	A value
9a	Me	251	14.9	233	−6.6	21.5
9b	Et	251	13.5	233	−5.9	19.4
9c	*n*-Pr	251	12.9	235	−5.8	18.7
9d	i-Pr	252	10.9	232	−5.4	16.3
9e	Cy	252	9.8	229	−4.4	14.2
9f	*t*-Bu	250	7.1	232	−4.1	11.2

Fig. 5 Sign of the pairwise interaction between the chromophores at the 4 and 6 positions in the *gg*, *gt* and *tg* rotamers.
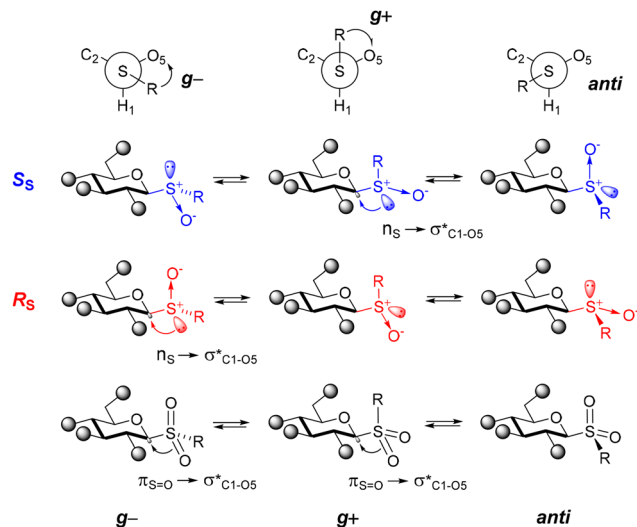

Fig. 6 Staggered *g−*, *g+*, and *anti* conformers about the ϕ (C−S−C1−O5) torsion angle for glucosyl sulfoxides and sulfones and the nomenclature used herein.
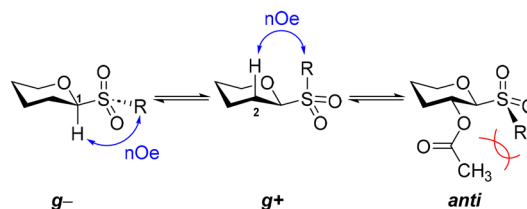

Fig. 7 Expected nOe couplings between H1 and the aglycone's protons closer to the sulfur.

4d, and the *tert*-butyl's methyl groups in **4f**, whose signals were well isolated in the respective ^{1}H NMR spectrum on both tested solvents, allowing for selective irradiation.

In the apolar media (C$_6$D$_6$), we observe that methyl and ethyl derivatives **4a** and **4b** show strong nOe couplings with H2 and a weak interaction with H1, suggesting that in these small-aglycone-carrying sulfones, the *g+* rotamer predominates the conformation about ϕ. As the aglycone increases its degree of substitution, the intensity of the nOe peak with H2 decreases and that with H1 increases. Thus, iso-propyl sulfone **4d** shows comparable nOe intensities between H1 and H2 nOe peaks, suggesting an equilibrium between the *g−* and *g+* conformers. In *tert*-butyl sulfone **4f**, the larger nOe peak with H1 suggests a ϕ torsion largely predominated by the *g−* conformer. No nOe spatial couplings with the acetyl group at C2 were observed upon irradiation of the above-mentioned protons.

In CD$_3$CN, the conformation about ϕ shows a different pattern, especially for those glucosyl sulfones carrying smaller alkyl substituents. Thus, we observe that derivatives **4a** and **4b** exhibit comparable intensities on the H1 and H2 nOe peaks, which points to a glycosidic ϕ conformation distributed between the *g−* and *g+* rotamers. The iso-propyl glucoside **4d** shows nOe peaks with H1 and H2, with H1 being the most
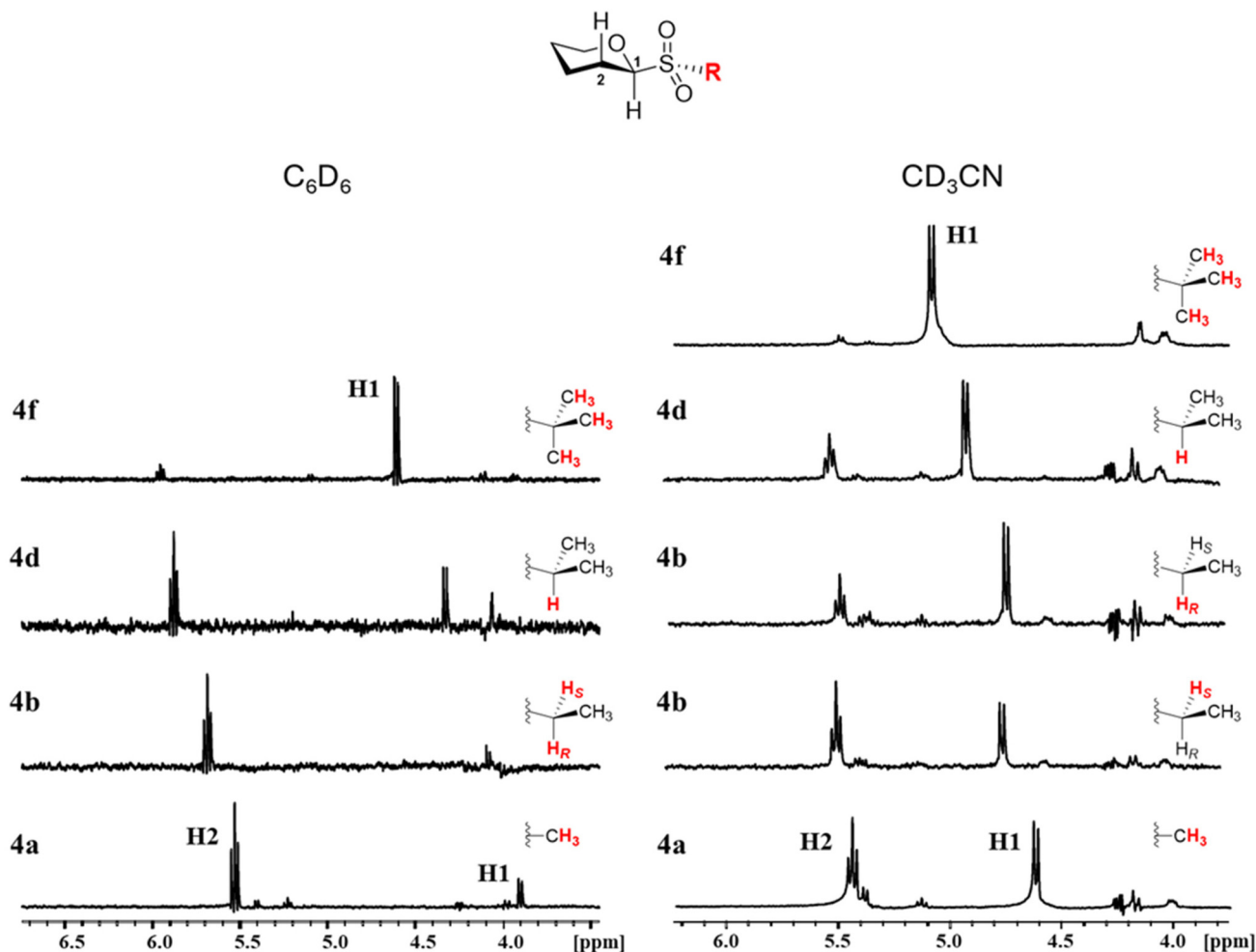
7006 | *Org. Biomol. Chem.*, 2025, **23**, 7000–7012

This journal is © The Royal Society of Chemistry 2025

Fig. 8 Stacked 1D-NOESY spectra for glucosyl sulfones **4a** (R = Me), **4b** (R = Et), **4d** (R = i-Pr), and **4f** (R = *t*-Bu) in C_6D_6 (A) and CD_3CN (B). Irradiated hydrogens are highlighted in red.

intense, suggesting a preference for the *g*− conformer. In *tert*-butyl sulfone **4f**, the largely predominant H1 nOe peak evidences a glycosidic conformation anchored in *g*−. Thus, the effect of the media polarity over the glycosidic bond conformation seems to be more relevant in glycosides carrying small alkyl substituents, where we observe higher flexibilities. As the aglycone substituent's size increases, the glycosidic bond becomes stiffer and anchored in *g*− in both polar and apolar media, likely due to the steric repulsions with H2 which destabilize *g*+.
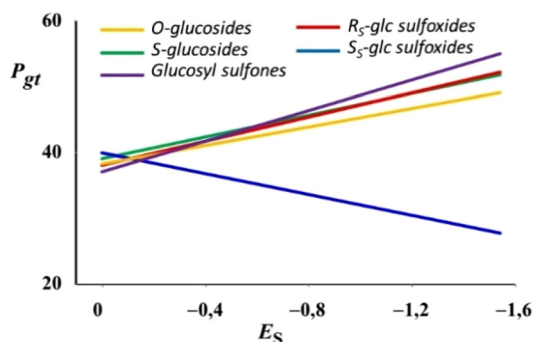
Conclusions

Herein we have shown by means of NMR and CD spectroscopy that the rotamer populations of the hydroxymethyl group in alkyl glucosyl sulfones depend on the structural nature of the aglycone. Thus, in both synthetic models, an increment in the alkyl substituent's bulkiness leads to progressive increments in *gt* contributions at the expense of *gg*. In addition, as the Charton value (ν) increases, the *gt* population linearly increases at the expense of the *gg* population.

These results are like those obtained with alkyl *O*-,[8] *S*-,[9] and *C*-[10] glycosides as well as R_S glucosyl sulfoxides, but opposite to those from the S_S glucosyl sulfoxides.[11] All these studies pointed to different values of the stereoelectronic *exo*-anomeric

Fig. 9 P_{gt} versus alkyl's Taft's values (E_s) for alkyl *O*-glucosides, thioglucosides, glucosyl sulfoxides and sulfones.

This journal is © The Royal Society of Chemistry 2025

Org. Biomol. Chem., 2025, **23**, 7000–7012 | **7007**

effect to be responsible for this behavior. In addition, the independent conformational properties of carbasugars[12] of the aglycone reveal that the endocyclic oxygen is involved and it is necessary for this relationship.

Fig. 9 shows the general behavior of P_{gt} versus Taft's steric parameter (E_S) of the alkyl group attached to O-, S-, R_S and S_S sulfinyl as well as sulfonyl groups in CDCl₃. It can be observed that in all cases but the S_S glucosyl sulfoxides, an increase in the absolute value of E_S leads to larger gt populations. Therefore, it seems that the conformational properties of the hydroxymethyl group of ester-protected alkyl glucosyl sulfones are also directly related to the stereoelectronic exo-anomeric effect.

Opposite to the sulfinyl group, the sulfonyl group possesses higher π character in the S=O bond.[29] This property could give rise to a $\pi_{S=O} \rightarrow \sigma^*_{C1-O5}$ interaction that, in a similar way to other glycosides, led to the existence of the exo-anomeric effect in alkyl glucosyl sulfones. Either the $g-$ or the $g+$ conformation fulfills the spatial requirements for the $\pi_{S=O} \rightarrow \sigma^*_{C1-O5}$ interaction to take place.

The nOe study on the conformational patterns about the glycosidic bond ϕ (H1–C1–S–C) revealed its dependency on the aglycone's nature. As the alkyl substituent increases its degree of substitution, the intensity of the nOe peak with H2 decreases and that with H1 increases, meaning that the $g-$ conformer increases its predominance at the expense of $g+$.

The solvent polarity exerts an important influence over the conformational pattern of the glycosidic bond and a less pronounced one over the hydroxymethyl group's flexibility. In apolar media (C₆D₆), glycosides carrying small aglycones exhibit a glycosidic conformation markedly predominated by $g+$, whereas in a polar solvent (CD₃CN), the glycosidic bond becomes more flexible with comparable $g+$ and $g-$ distributions. In both polar and apolar media, we observe the same hydroxymethyl conformational trends with comparable P_{gg}, P_{gt}, and P_{tg} values in both glycoside series studied.

Experimental

General information

NMR spectra were recorded in Bruker AVANCE 400, 500 and 600 spectrometers. Mono-dimensional ¹H NMR spectra were collected at 400, 500 and 600 MHz and 1D ¹³C NMR spectra were collected at 100 and 150 MHz, VTU 300.0 °K. Chemical shifts are reported in parts per million (ppm). The residual solvent peak was used as an internal reference. FIDs were processed using Bruker TopSpin software by applying a Fourier transform with phase correction combined with exponential multiplication (efp command). The $^3J_{H,H}$ coupling constants were measured directly from the peak's chemical shift differences of the resulting spectra or using the distance measurement tool in TopSpin. The H5,H6 coupling constants (ABX system) were obtained (i) by direct measurement of the lines of H6R, H6S, or H5 in spectrometers of different magnetic field strengths (from 400 to 600 MHz) and (ii) by simulating each

spectrum by using Bruker's simulation and iteration tool (DAISY) available in TopSpin 4.0.7 (see ESI Tables S2–S4 and Fig. S26–S45†).[30]

HRMS spectra were analyzed by TOF MS ES+. For analytical and preparative thin-layer chromatography, silica gel ready-foils and glass-backed plates (1 mm) were used, respectively, being developed with 254 nm UV light and/or spraying with AcOH/H₂O/H₂SO₄ (80 : 16 : 4) and heating at 150 °C. Column chromatography was performed using silica gel (0.015–0.04 mm) and n-hexane/EtOAc solvent systems. All reagents were obtained from commercial sources and used without further purification. Solvents were dried and distilled before use.

For general procedures for the synthesis and characterization of the alkyl β-D-thioglucopyranosides **3a**, **3b**, and **3(d–f)** and **8(a–f)**, see ref. 9, 13 and 14. For compound **3c**, see the following section.

n-Propyl 2,3,4,6-tetra-O-acetyl-1-thio-β-D-glucopyranoside (3c)

To a stirred solution of 1,2,3,4,6-penta-O-acetyl-β-D-glucopyranose (855 mg, 2.2 mmol) and propanothiol (2 eq., 0.40 mL) in dry dichloromethane (5 mL mmol⁻¹) at room temperature and under an N₂ atmosphere, boron trifluoride etherate (0.1 eq.) was added dropwise. The reaction progress was followed by TLC. When the starting compound was consumed, it was quenched by the addition of Et₃N and diluted with CH₂Cl₂. The organic layer was washed with brine, dried over anhydrous Na₂SO₄, and concentrated under reduced pressure. The product was purified by chromatography using silica gel and n-hexane/ethyl acetate as the eluent to afford the n-propyl thioglucoside **3c** (818 mg, 1.5 mmol, 92%). R_f: 0.43 (n-hex/EtOAc 3 : 2); [α]$_D$: −27.4 (c 1.2, CHCl₃); HRMS (FAB): calcd for C₁₇H₂₆O₉NaS [M + Na]⁺: 429.1195, found: 429.1190; ¹H NMR (δ, 400 MHz, CDCl₃): 5.21 (dd, J = 9.4 and 9.4 Hz, H-3), 5.07 (dd, J = 9.4 and 9.4 Hz, H-4), 5.02 (dd, J = 9.7 and 9.7 Hz, H-2), 4.47 (d, J = 10.0 Hz, H-1), 4.23 (dd, J = 5.0 and 12.3 Hz, H-6R), 4.12 (dd, J = 2.2 and 12.3 Hz, H-6S), 3.69 (ddd, J = 2.2, 5.0 and 9.8 Hz, H-5), 2.71–2.57 (m, 2H), 2.07 (s, 3H), 2.05 (s, 3H), 2.01 (s, 3H), 1.99 (s, 3H), 1.67–1.57 (m, 2H), 0.97 (dd, J = 7.3 and 7.3 Hz, 3H); ¹³C NMR (δ, CDCl₃): 170.6 (s), 170.2 (s), 169.4 (s), 169.3 (s), 83.7 (d, C-1), 75.8 (d, C-5), 73.9 (d, C-3), 69.9 (d, C-2), 68.4 (d, C-4), 62.2 (t, C-6), 32.1 (t), 23.1 (q), 20.7 (q), 20.6 (q), 20.5 (q), 13.4 (q); E.A.: calcd for C₁₇H₂₆O₉S: C, 50.24; H, 6.45; S, 7.89, found: C, 50.34; H, 6.60; S, 7.78.

General procedure for the oxidation of alkyl S-glycosides to alkyl glycosyl sulfones

Alkyl S-glucoside (1.0 equiv.), Ac₂O (3.0 equiv.), and SiO₂ (200 mg mmol⁻¹ of S-glucoside) were suspended in DCM (5.0 ml mmol⁻¹ of S-glucoside), and H₂O₂ (3.0 equiv., from a 35% in H₂O solution) was added at room temperature and under vigorous stirring. The reaction was maintained under stirring until achieving complete oxidation of the starting material (TLC analysis). The system was then diluted with DCM, filtered through filter paper to remove SiO₂, and the filtrate was transferred to a separation funnel and subsequently

7008 | Org. Biomol. Chem., 2025, **23**, 7000–7012

This journal is © The Royal Society of Chemistry 2025

washed with 10% $Na_2S_2O_3$, $NaHCO_3$ (sat.), and brine. The organic layer was collected, dried over Na_2SO_4, filtered, and concentrated in a rotary evaporator. The resulting crude was then purified by normal phase flash chromatography using mixtures of ethyl acetate and *n*-hexane as the eluent system in proportions according to the sulfone's polarity.

2,3,4,6-Tetra-*O*-acetyl-1-(methylsulfonyl)-β-D-glucopyranoside (4a)

Following the general procedure for the synthesis of alkyl glycosyl sulfones, methyl *S*-glucoside **3a** (83 mg, 0.22 mmol) afforded glycosyl sulfone **4a** (90 mg, 0.219 mmol, 99%) as a white solid. R_f: 0.33 (*n*-hex/EtOAc 2:3); $[\alpha]_D$: −2.7 (c 0.9, CHCl$_3$); ^{1}H NMR (δ, 400 MHz, CDCl$_3$): 5.42 (dd, *J* = 9.6 and 9.6 Hz, H-2), 5.30 (dd, *J* = 9.3 and 9.3 Hz, H-3), 5.12 (dd, *J* = 9.7 and 9.7 Hz, H-4), 4.35 (d, *J* = 9.9 Hz, H-1), 4.32 (dd, *J* = 4.8 and 12.7 Hz, H-6*R*), 4.20 (dd, *J* = 2.2 and 12.7 Hz, H-6*S*), 3.85 (ddd, *J* = 2.2, 4.8, and 10.0 Hz, H-5), 2.95 (s, 3H), 2.08 (s, 3H), 2.06 (s, 3H), 2.03 (s, 3H), 2.02 (s, 3H); ^{13}C{^{1}H} NMR (δ, 100 MHz, CDCl$_3$): 170.4 (s), 169.9 (s), 169.5 (s), 169.2 (s), 88.4 (d, C-1), 76.8 (d, C-5), 73.0 (d, C-3), 67.4 (d, C-4), 66.7 (d, C-2), 61.3 (d, C-6), 36.4 (q), 20.6 (q), 20.6 (q), 20.5 (q), 20.4 (q). HRMS (FAB): calcd for $C_{15}H_{22}O_{11}S$ Na $[M + Na]^+$: 433.0781, found: 433.0770.

2,3,4,6-Tetra-*O*-acetyl-1-(ethylsulfonyl)-β-D-glucopyranoside (4b)

Following the general procedure for the synthesis of alkyl glycosyl sulfones, ethyl *S*-glucoside **3b** (115 mg, 0.29 mmol) afforded glycosyl sulfone **4b** (119 mg, 0.28 mmol, 97%) as a white solid. R_f: 0.37 (*n*-hex/EtOAc 2:3); $[\alpha]_D$: −9.6 (c 0.3, CHCl$_3$); ^{1}H NMR (δ, 400 MHz, CDCl$_3$): 5.49 (dd, *J* = 9.6 and 9.6 Hz, H-2), 5.31 (dd, *J* = 9.4 and 9.4 Hz, H-3), 5.12 (dd, *J* = 9.8 and 9.8 Hz, H-4), 4.46 (d, *J* = 9.9 Hz, H-1), 4.26 (dd, *J* = 4.7 and 12.7 Hz, H-6*R*), 4.21 (dd, *J* = 2.1 and 12.7 Hz, H-6*S*), 3.83 (ddd, 2.1, 4.7, and 9.2 Hz, H-5), 3.14 (m, 2H), 2.08 (s), 2.07 (s), 2.04 (s), 2.03 (s), 1.40 (dd, *J* = 7.5 and 7.5 Hz, 3H); ^{13}C{^{1}H} NMR (δ, 100 MHz, CDCl$_3$): 170.4 (s), 170.0 (s), 169.3 (s), 169.2 (s), 87.5 (d, C-1), 76.8 (d, C-5), 73.1 (d, C-3), 67.4 (d, C-4), 66.5 (d, C-2), 61.4 (t, C-6), 43.9 (t), 20.6 (q), 20.6 (q), 20.5 (q), 20.4 (q), 5.4 (q); HRMS (FAB): calcd for $C_{16}H_{25}O_{11}S$ $[M + H]^+$: 425.1118, found: 425.1133.

2,3,4,6-Tetra-*O*-acetyl-1-(*n*-propylsulfonyl)-β-D-glucopyranoside (4c)

Following the general procedure for the synthesis of alkyl glycosyl sulfones, *n*-propyl *S*-glucoside **3c** (91 mg, 0.22 mmol) afforded sulfone **4c** (92 mg, 0.21 mmol, 95%) as a white solid. R_f: 0.47 (*n*-hex/EtOAc 2:3); $[\alpha]_D$: −17.2 (c 0.9, CHCl$_3$); ^{1}H NMR (δ, 400 MHz, CDCl$_3$): 5.47 (dd, *J* = 9.6 and 9.6 Hz, H-2), 5.30 (dd, *J* = 9.3 and 9.3 Hz, H-3), 5.11 (dd, *J* = 9.7 and 9.7 Hz, H-4), 4.42 (d, *J* = 9.9 Hz, H-1), 4.26 (dd, *J* = 4.8 and 12.6 Hz, H-6*R*), 4.20 (dd, *J* = 2.3 and 12.6 Hz, H-6*S*), 3.82 (ddd, *J* = 2.3, 4.8, and 10.0 Hz, H-5), 3.08 (m, 2H), 2.08 (s, 3H), 2.06 (s, 3H), 2.03 (s, 3H), 2.02 (s, 3H), 1.90 (m, 2H), 1.09 (dd, *J* = 7.4 and 7.4 Hz, 3H); ^{13}C{^{1}H} NMR (δ, 100 MHz, CDCl$_3$): 170.4 (s), 170.0 (s), 169.3 (s), 169.2 (s), 87.8 (d, C-1), 76.7 (d, C-5), 73.1 (d, C-3),

67.4 (d, C-4), 66.4 (d, C-2), 61.4 (t, C-6), 50.9 (t), 20.6 (q), 20.6 (q), 20.5(q), 20.5(q), 14.7 (t), 13.2 (q); HRMS (FAB): calcd for $C_{17}H_{26}O_{11}SNa$ $[M + Na]^+$: 461.1094, found: 461.1075.

2,3,4,6-Tetra-*O*-acetyl-1-(iso-propylsulfonyl)-β-D-glucopyranoside (4d)

Following the general procedure for the synthesis of alkyl glycosyl sulfones, iso-propyl *S*-glucoside **3d** (95 mg, 0.23 mmol) afforded sulfone **4d** (92 mg, 0.21 mmol, 91%) as a white solid. R_f: 0.38 (*n*-hex/EtOAc 2:3); $[\alpha]_D$: −12.4 (c 0.9, CHCl$_3$); ^{1}H NMR (δ, 600 MHz, CDCl$_3$): 5.56 (dd, *J* = 9.6 and 9.6 Hz, H-2), 5.33 (dd, *J* = 9.6 and 9.6 Hz, H-3), 5.11 (dd, *J* = 9.6 and 9.6 Hz, H-4), 4.63 (d, *J* = 9.6 Hz, H-1), 4.23 (dd, *J* = 2.4 and 12.6 Hz, H-6*S*), 4.20 (dd, *J* = 4.8 and 12.6 Hz, H-6*R*), 3.80 (ddd, *J* = 2.4, 4.8, and 9.6 Hz, H-5), 3.48 (m, 1H), 2.08 (s, 3H), 2.06 (s, 3H), 2.04 (s, 3H), 2.03 (s, 3H), 1.39 (d, *J* = 7.2 Hz, 3H), 1.37 (d, *J* = 7.2 Hz, 3H); ^{13}C{^{1}H} NMR (δ, 100 MHz, CDCl$_3$): 170.3 (s), 170.1 (s), 169.2 (s), 169.0 (s), 85.9 (d, C-1), 76.7 (d, C-5), 73.2 (d, C-3), 67.5 (d, C-4), 66.5 (d, C-2), 61.6 (t, C-6), 51.2 (d), 20.6 (q), 20.6 (q), 20.5(q), 20.4(q), 16.1 (q), 13.4 (q); HRMS (FAB): calcd for $C_{17}H_{26}O_{11}SNa$ $[M + Na]^+$: 461.1094, found: 461.1092.

2,3,4,6-Tetra-*O*-acetyl-1-(cyclohexylsulfonyl)-β-D-glucopyranoside (4e)

Following the general procedure for the synthesis of alkyl glycosyl sulfones, cyclohexyl *S*-glucoside **3e** (101 mg, 0.25 mmol) afforded sulfone **4e** (110 mg, 0.23 mmol, 94%) as a white solid. R_f: 0.52 (*n*-hex/EtOAc 2:3); $[\alpha]_D$: −14.6 (c 1.2, CHCl$_3$); ^{1}H NMR (δ, 400 MHz, CDCl$_3$): 5.55 (dd, *J* = 9.7 and 9.7 Hz, H-2), 5.32 (dd, *J* = 9.4 and 9.4 Hz, H-3), 5.07 (dd, *J* = 9.5 and 9.5 Hz, H-4), 4.60 (d, *J* = 9.8 Hz, H-1), 4.22 (dd, *J* = 2.3 and 12.5 Hz, H-6*S*), 4.16 (dd, *J* = 5.6 and 12.5 Hz, H-6*R*), 3.78 (ddd, *J* = 2.3, 5.6, and 10.1 Hz, H-5), 3.24 (m, 1H), 2.16 (m, 2H), 2.07 (s, 3H), 2.03 (s, 3H), 2.02 (s, 3H), 2.01 (s, 3H), 1.60 (m, 4H), 1.26 (m, 4H); ^{13}C{^{1}H} NMR (δ, 100 MHz, CDCl$_3$): 170.3 (s), 170.1 (s), 169.2 (s), 169.0 (s), 85.7 (d, C-1), 76.7 (d, C-5), 73.2 (d, C-3), 67.5 (d, C-4), 66.3 (d, C-2), 61.8 (t, C-6), 58.9 (d), 25.9 (t), 25.1 (t), 25.0 (t), 25.0 (t), 22.8 (t), 20.6 (q), 20.5 (q), 20.5(q), 20.4(q); HRMS (ESI): calcd for $C_{20}H_{30}O_{11}NaS$ $[M + Na]^+$: 501.1422, found: 501.1407.

2,3,4,6-Tetra-*O*-acetyl-1-(*tert*-butylsulfonyl)-β-D-glucopyranoside (4f)

Following the general procedure for the synthesis of alkyl glycosyl sulfones, *tert*-butyl *S*-glucoside **3f** (110 mg, 0.26 mmol) afforded sulfone **4f** (116 mg, 0.25 mmol, 96%) as a white solid. R_f: 0.40 (*n*-hex/EtOAc 2:3); ^{1}H NMR (δ, 400 MHz, CDCl$_3$): 5.58 (dd, *J* = 9.3 and 9.3 Hz, H-2), 5.34 (dd, *J* = 9.3 and 9.3 Hz, H-3), 5.06 (dd, *J* = 9.8 and 9.8 Hz, H-4), 4.84 (d, *J* = 9.7 Hz, H-1), 4.24 (dd, *J* = 2.4 and 12.5 Hz, H-6*S*), 4.13 (dd, *J* = 6.5 and 12.5 Hz, H-6*R*), 3.80 (ddd, *J* = 2.4, 6.5, and 9.4 Hz, H-5), 2.07 (s, 3H), 2.06 (s, 3H), 2.04 (s, 3H), 2.03 (s, 3H), 1.47 (m, 9H); ^{13}C{^{1}H} (δ, 100 MHz, CDCl$_3$): 170.2 (s), 170.1 (s), 169.2 (s), 168.9 (s), 86.3 (d, C-1), 76.5 (d, C-5), 73.2 (d, C-3), 67.7 (d, C-4), 66.5 (d, C-2), 62.6 (t, C-6), 62.1 (s), 23.9 (q, ×3C),

This journal is © The Royal Society of Chemistry 2025

Org. Biomol. Chem., 2025, **23**, 7000–7012 | 7009

20.6 (q), 20.6 (q), 20.5 (q), 20.4 (q); HRMS (FAB): calcd for $C_{18}H_{29}O_{11}S$ [M + H]$^+$: 453.1431, found: 453.1405.

2,3-Di-*O*-acetyl-4,6-bis-*O*-(4-bromobenzoyl)-1-(methylsulfonyl)-β-D-glucopyranoside (9a)

Following the general procedure for the synthesis of alkyl glycosyl sulfones, methyl *S*-glucoside **8a** (18 mg, 0.03 mmol) afforded sulfone **9a** (19 mg, 0.027 mmol, 92%) as a white solid. R_f: 0.43 (*n*-hex/EtOAc 1 : 1); [α]$_D$: +9.4 (c 0.2, CHCl$_3$); ^{1}H NMR (δ, 400 MHz, CDCl$_3$): 7.81 (m, 4H), 7.56 (m, 4H), 5.53 (m, H-2 and H-3), 5.45 (dd, *J* = 9.7 and 9.7 Hz, H-4), 4.61 (dd, *J* = 3.0 and 12.5 Hz, H-6*S*), 4.47 (d, *J* = 9.4 Hz, H-1), 4.44 (dd, *J* = 4.9 and 12.5 Hz, H-6*R*), 4.13 (ddd, *J* = 3.0, 4.9, and 9.7 Hz, H-5), 2.97 (s, 3H), 2.09 (s, 3H), 1.93 (s, 3H). ^{13}C{^{1}H} NMR (δ, 100 MHz, CDCl$_3$): 170.1 (s), 169.5 (s), 165.7 (s), 164.5 (s), 132.1 (d, ×2C), 131.9 (d, ×2C), 131.3 (s, ×2C), 131.1 (s, ×2C), 129.4 (s), 128.7 (s), 128.0 (s), 127.1 (s), 88.5 (d, C-1), 76.9 (d, C-5), 72.6 (d, C-3), 68.7 (d, C-4), 66.7 (d, C-2), 62.5 (t, C-6), 36.6 (q), 20.6 (q), 20.4 (q); HRMS (FAB): calcd for $C_{25}H_{24}$ Br$_2O_{11}$SNa [M + Na]$^+$: 712.9304, found: 712.9293; UV (CH$_3$CN) λ$_{max}$ nm (ε): 245 (ε 38 200); CD (CH$_3$CN) λ$_{ext}$ nm (Δε): 251 (14.9), 233 (−6.6).

2,3-Di-*O*-acetyl-4,6-bis-*O*-(4-bromobenzoyl)-1-(ethylsulfonyl)-β-D-glucopyranoside (9b)

Following the general procedure for the synthesis of alkyl glycosyl sulfones, ethyl *S*-glucoside **8b** (19 mg, 0.03 mmol) afforded sulfone **9b** (20 mg, 0.028 mmol, 95%) as a white solid: R_f: 0.47 (*n*-hex/EtOAc 1 : 1); [α]$_D$: +8.6 (c 0.1, CHCl$_3$); ^{1}H NMR (δ, 400 MHz, CDCl$_3$): 7.81 (m, 4H), 7.58 (m, 4H), 5.59 (dd, *J* = 9.1 and 9.1 Hz, H-4), 5.55 (dd, *J* = 9.0 and 9.0 Hz, H-3), 5.44 (dd, *J* = 9.5 and 9.5 Hz, H-4), 4.58 (d, *J* = 9.6 Hz, H-1), 4.60 (dd, *J* = 3.0 and 12.1 Hz, H-6*S*), 4.43 (dd, *J* = 5.3 and 12.1 Hz, H-6*R*), 4.11 (ddd, *J* = 3.0, 5.3, and 9.3 Hz, H-5), 3.15 (m, 2H), 2.08 (s, 3H), 1.93 (s, 3H), 1.36 (dd, *J* = 7.5 and 7.5 Hz, 3H); ^{13}C{^{1}H} NMR (δ, 100 MHz, CDCl$_3$): 169.7 (s), 169.1 (s), 164.9 (s), 164.1 (s), 131.9 (d, ×2C), 131.7 (d, ×2C), 131.1 (d, ×2C), 130.9 (d, ×2C), 129.2 (s), 128.6 (s), 127.8 (s), 126 (s), 87.4 (d, C-1), 76.9 (d, C-5), 72.5 (d, C-3), 68.5 (d, C-4), 66.2 (d, C-2), 62.3 (t, C-6), 29.5 (t), 20.4 (q), 20.2 (q), 5.4 (q); HRMS (ESI) calcd for $C_{26}H_{26}O_{11}$NaSBr$_2$ [M + Na]$^+$: 726.9460, found: 726.9479; UV (CH$_3$CN) λ$_{max}$ nm (ε): 245 (ε 38 200); CD (CH$_3$CN) λ$_{ext}$ nm (Δε): 251 (13.5), 233 (−5.9).

2,3-Di-*O*-acetyl-4,6-bis-*O*-(4-bromobenzoyl)-1-(*n*-propylsulfonyl)-β-D-glucopyranoside (9c)

Following the general procedure for the synthesis of alkyl glycosyl sulfones, *n*-propyl *S*-glucoside **8c** (33 mg, 0.05 mmol) afforded sulfone **9c** (35 mg, 0.049 mmol, 98%) as a white solid. R_f: 0.53 (*n*-hex/EtOAc 1 : 1); [α]$_D$: +6.4 (c 0.3, CHCl$_3$); ^{1}H NMR (δ, 400 MHz, CDCl$_3$): 7.85–7.80 (m, 4H), 7.60–7.55 (m, 4H), 5.59 (dd, *J* = 9.1 and 9.1 Hz, H-2), 5.55 (dd, *J* = 9.3 and 9.3 Hz, H-3), 5.43 (dd, *J* = 9.5 and 9.5 Hz, H-4), 4.60 (dd, *J* = 3.0 and 12.5 Hz, H-6*S*), 4.54 (d, *J* = 9.4 Hz, H-1), 4.44 (dd, *J* = 5.4 and 12.5 Hz, H-6*R*), 4.11 (ddd, *J* = 3.0, 5.4, and 9.5 Hz, H-5), 3.13–3.03 (m, 2H), 2.09 (s, 3H), 2.05 (s, 3H), 1.94–1.80 (m, 2H), 1.03 (dd, *J* = 7.5 and 7.5 Hz, 3H); ^{13}C{^{1}H} NMR (δ, 100 MHz, CDCl$_3$): 169.9 (s), 169.3 (s), 165.1 (s), 164.3 (s), 132.1 (d), 131.9 (d), 131.3 (d), 131.1 (d), 129.4 (s), 128.7 (s), 128.0 (s), 127.1 (s), 87.8 (d, C-1), 77.2 (d, C-5), 72.7 (d, C-3), 68.7 (d, C-4), 66.4 (d, C-2), 62.6 (t, C-6), 51.1 (t), 20.6 (q), 20.4 (q), 14.8 (t), 13.2 (q); HRMS (ESI): calcd for $C_{27}H_{28}O_{11}$NaSBr$_2$ [M + Na]$^+$: 742.9596, found: 742.9591; UV (CH$_3$CN) λ$_{max}$ nm (ε): 245 (ε 38 200); CD (CH$_3$CN) λ$_{ext}$ nm (Δε): 251 (12.9), 235 (−5.8).

2,3-Di-*O*-acetyl-4,6-bis-*O*-(4-bromobenzoyl)-1-(iso-propylsulfonyl)-β-D-glucopyranoside (9d)

Following the general procedure for the synthesis of alkyl glycosyl sulfones, iso-propyl *S*-glucoside **8d** (36 mg, 0.05 mmol) afforded sulfone **9d** (33 mg, 0.046 mmol, 92%) as a white solid. R_f: 0.50 (*n*-hex/EtOAc 1 : 1); [α]$_D$: −6.4 (c 0.4, CHCl$_3$) ^{1}H NMR (δ, 400 MHz, CDCl$_3$): 7.81 (m, 4H), 7.56 (m, 4H), 5.65 (dd, *J* = 9.4 and 9.4 Hz, H-2), 5.57 (dd, *J* = 9.3 and 9.3 Hz, H-3), 5.40 (dd, *J* = 9.8 and 9.8 Hz, H-4), 4.74 (d, *J* = 9.6 Hz, H-1), 4.56 (dd, *J* = 2.7 and 12.4 Hz, H-6*S*), 4.43 (dd, *J* = 5.8 and 12.4 Hz, H-6*R*), 4.09 (ddd, *J* = 2.7, 5.8, and 9.0 Hz, H-5), 3.47 (m, 1H), 2.07 (s, 3H), 1.92 (s, 3H), 1.36 (d, *J* = 7.0 Hz, 3H), 1.30 (d, *J* = 7.0 Hz, 3H); ^{13}C{^{1}H} NMR (δ, 100 MHz, CDCl$_3$): 170.1 (s), 169.1 (s), 165.1 (s), 164.3 (s), 132.1 (d, ×2), 131.9 (d, ×2), 131.3 (d), 131.1 (d, ×2), 129.3 (s), 128.8 (s), 127.9 (s), 127.1 (s), 85.8 (d, C-1), 76.6 (d, C-5), 72.3 (d, C-3), 68.8 (d, C-4), 66.5 (d, C-2), 62.7 (t, C-6), 51.2 (d), 20.6 (q), 20.5 (q), 16.2 (q), 13.3 (q); HRMS (FAB): calcd for $C_{27}H_{28}O_{11}$NaSBr$_2$ [M + Na]$^+$: 742.9596, found: 742.9551; UV (CH$_3$CN) λ$_{max}$ nm (ε): 244 nm (ε 38 200); CD (CH$_3$CN) λ$_{ext}$ nm (Δε): 252 (10.9), 232 (−5.8).

2,3-Di-*O*-acetyl-4,6-bis-*O*-(4-bromobenzoyl)-1-(cyclohexylsulfonyl)-β-D-glucopyranoside (9e)

Following the general procedure for the synthesis of alkyl glycosyl sulfones, cyclohexyl *S*-glucoside **8e** (71 mg, 0.1 mmol) afforded sulfone **9e** (70 mg, 0.093 mmol, 93%) as a white solid. R_f: 0.58 (*n*-hex/EtOAc 1 : 1); [α]$_D$: −8.3 (c 0.5, CHCl$_3$); ^{1}H NMR (δ, 400 MHz, CDCl$_3$): 7.82 (m, 4H), 7.57 (m, 4H), 5.66 (dd, *J* = 9.4 and 9.4 Hz, H-2), 5.55 (dd, *J* = 9.4 and 9.4 Hz, H-3), 5.39 (dd, *J* = 9.8 and 9.8 Hz, H-4), 4.70 (d, *J* = 9.6 Hz, H-1), 4.55 (dd, *J* = 2.4 and 12.5 Hz, H-6*S*), 4.42 (dd, *J* = 5.9 and 12.5 Hz, H-6*R*), 4.08 (ddd, *J* = 2.4, 5.9, and 9.6 Hz, H-5), 3.24 (m, 1H), 2.17 (m, 2H), 2.07 (s, 3H), 1.98 (s, 3H), 1.56 (m, 4H), 1.20 (m, 4H); ^{13}C{^{1}H} NMR (δ, 100 MHz, CDCl$_3$): 170.1 (s), 169.1 (s), 165.1 (s), 164.3 (s), 132.1 (d, ×2), 131.9 (d, ×2), 131.3 (d, ×2C), 131.1 (d, ×2), 129.3 (s), 128.8 (s), 127.9 (s), 127.3 (s), 85.6 (d, C-1), 76.7 (d, C-5), 72.8 (d, C-3), 68.7 (d, C-4), 66.3 (d, C-2), 62.8 (t, C-6), 58.9 (d), 25.9 (t), 25.0 (t), 24.9 (t), 24.7 (t), 22.7 (t), 20.6 (q), 20.5 (q); HRMS (FAB): calcd for $C_{30}H_{32}O_{11}$NaSBr$_2$ [M + Na]$^+$: 780.9930, found: 780.9948; UV (CH$_3$CN) λ$_{max}$ nm (ε): 244 nm (ε 38 200); CD (CH$_3$CN) λ$_{ext}$ nm (Δε): 252 (9.8), 229 (−4.4).

2,3-Di-*O*-acetyl-4,6-bis-*O*-(4-bromobenzoyl)-1-(*tert*-butylsulfonyl)-β-D-glucopyranoside (9f)

Following the general procedure for the synthesis of alkyl glycosyl sulfones, *tert*-butyl *S*-glucoside **8f** (106 mg, 0.15 mmol) afforded sulfone **9f** (99 mg, 0.14 mmol, 93%) as a white solid.

7010 | *Org. Biomol. Chem.*, 2025, **23**, 7000–7012

This journal is © The Royal Society of Chemistry 2025

R_f: 0.52 (*n*-hex/EtOAc 1 : 1); $[\alpha]_D$: −15.2 (c 0.8, CHCl$_3$); ^{1}H NMR (δ, 400 MHz, CDCl$_3$): 7.81 (m, 4H), 7.57 (m, 4H), 5.69 (dd, J = 9.2 and 9.2 Hz, H-2), 5.58 (dd, J = 9.1 and 9.1 Hz, H-3), 5.36 (dd, J = 9.6 and 9.6 Hz, H-4), 4.95 (d, J = 9.5 Hz, H-1), 4.58 (dd, J = 2.6 and 12.2 Hz, H-6S), 4.39 (dd, J = 6.8 and 12.2 Hz, H-6R), 4.12 (ddd, J = 2.6, 6.8, and 9.9 Hz, H-5), 2.07 (s, 3H), 1.94 (s, 3H), 1.44 (s, 9H); ^{13}C{^{1}H} (δ, 100 MHz, CDCl$_3$): 170.1 (s), 169.0 (s), 165.1 (s), 164.4 (s), 132.1 (d, ×2C), 132.0 (d, ×2C), 131.3 (d, ×2C), 131.1 (d, ×2C), 129.3 (s), 128.8 (s), 127.9 (s), 127.1 (s), 86.4 (d, C-1), 76.5 (d, C-5), 72.8 (d, C-3), 68.8 (d, C-4), 66.5 (d, C-2), 63.2 (t, C-6), 62.6 (s), 23.9 (q, ×3C), 20.7 (q), 20.5 (q); HRMS (FAB): calcd for C$_{28}$H$_{30}$Br$_2$NaO$_{11}$S [M + Na]$^+$: 756.9753; found: 756.9787; UV (CH$_3$CN) λ_{max} nm (ε): 244 nm (ε 38 200); CD (CH$_3$CN) λ_{ext} nm ($\Delta\varepsilon$): 250 (7.1), 232 (−4.1).

Conflicts of interest

There are no conflicts to declare.

Data availability

All related data generated and/or analyzed during the current study are available from the corresponding author upon reasonable request.

Acknowledgements

References

1 A. Varki, *Glycobiology*, 2016, **27**(1), 3–49.

2 (*a*) P.-C. Pang, P. C. N. Chiu, C.-L. Lee, L.-Y. Chang, M. Panico, H. R. Morris, S. M. Haslam, K.-H. Khoo, G. F. Clark, W. S. B. Yeung and A. Dell, *Science*, 2011, **333**(6050), 1761–1764; (*b*) G. F. Clark, *Hum. Reprod.*, 2013, **28**(3), 566–577.

3 (*a*) J. D. Marth and P. K. Grewal, *Nat. Rev. Immunol.*, 2008, **8**(11), 874–887; (*b*) L. G. Baum and B. A. Cobb, *Glycobiology*, 2017, **27**(7), 619–624.

4 (*a*) L. Unione, A. Gimeno, P. Valverde, I. Calloni, H. Coelho, S. Mirabella, A. Poveda, A. Arda and J. Jimenez-Barbero, *Curr. Med. Chem.*, 2017, **24**(36), 4057–4080; (*b*) Y. Li, D. Liu, Y. Wang, W. Su, G. Liu and W. Dong, *Front. Immunol.*, 2021, 12; (*c*) R. Matos, I. Amorim, A. Magalhães, F. Haesebrouck, F. Gärtner and C. A. Reis, *Front. Mol. Biosci.*, 2021, 8.

5 (*a*) M. N. Christiansen, J. Chik, L. Lee, M. Anugraham, J. L. Abrahams and N. H. Packer, *Proteomics*, 2014, **14**(4–5), 525–546; (*b*) O. M. T. Pearce and H. Läubli, *Glycobiology*, 2015, **26**(2), 111–128; (*c*) S. S. Pinho and C. A. Reis, *Nat. Rev. Cancer*, 2015, **15**(9), 540–555; (*d*) D. Josic, T. Martinovic and K. Pavelic, *Electrophoresis*, 2019, **40**(1), 140–150.

6 (*a*) K. Dang, S. Jiang, Y. Gao and A. Qian, *Mol. Biol. Rep.*, 2022, **49**(8), 8037–8049; (*b*) M. Nauman and P. Stanley, *Biochem. Soc. Trans.*, 2022, **50**(2), 689–701; (*c*) A. R. Yale, E. Kim, B. Gutierrez, J. N. Hanamoto, N. S. Lav, J. L. Nourse, M. Salvatus, R. F. Hunt, E. S. Monuki and L. A. Flanagan, *Stem Cell Rep.*, 2023, **18**(6), 1340–1354; (*d*) J. C. Chatham and R. P. Patel, *Nat. Rev. Cardiol.*, 2024, **21**(8), 525–544.

7 B. Deore, R. W. Kwok, M. Toregeldiyeva, J. T. Vázquez, M. Marianski and C. A. Sanhueza, *J. Org. Chem.*, 2023, **88**(22), 15569–15579.

8 (*a*) C. Mayato, R. Dorta and J. T. Vázquez, *Tetrahedron: Asymmetry*, 2004, **15**(15), 2385–2397; (*b*) E. Q. Morales, J. I. Padron, M. Trujillo and J. T. Vázquez, *J. Org. Chem.*, 1995, **60**(8), 2537–2548; (*c*) J. I. Padrón and J. T. Vázquez, *Chirality*, 1997, **9**(5–6), 626–637; (*d*) J. I. Padrón, E. Q. Morales and J. T. Vázquez, *J. Org. Chem.*, 1998, **63**(23), 8247–8258; (*e*) C. Nóbrega and J. T. Vázquez, *Tetrahedron: Asymmetry*, 2003, **14**(18), 2793–2801.

9 (*a*) C. A. Sanhueza, R. L. Dorta and J. T. Vázquez, *Tetrahedron: Asymmetry*, 2008, **19**(2), 258–264; (*b*) B. Deore, J. E. Ocando, L. D. Pham and C. A. Sanhueza, *J. Org. Chem.*, 2022, **87**, 5952–5960.

10 (*a*) C. Mayato, R. L. Dorta and J. T. Vázquez, *Tetrahedron: Asymmetry*, 2007, **18**(8), 931–948; (*b*) C. Mayato, R. L. Dorta and J. T. Vázquez, *Tetrahedron: Asymmetry*, 2007, **18**(23), 2803–2811.

11 (*a*) C. A. Sanhueza, R. L. Dorta and J. T. Vázquez, *J. Org. Chem.*, 2011, **76**(19), 7769–7780; (*b*) C. A. Sanhueza, R. L. Dorta and J. T. Vázquez, *Tetrahedron: Asymmetry*, 2013, **24**(9), 582–593.

12 C. Mayato, R. L. Dorta, J. M. Palazón and J. T. Vázquez, *Carbohydr. Res.*, 2012, **352**, 101–108.

13 K. P. R. Kartha and R. A. Field, Synthesis and Activation of Carbohydrate Donors: Thioglycosides and Sulfoxides, in *Carbohydrates*, ed. H. Osborn, Elsevier Sciences Ltd, Oxford, 2023; pp. 121–145.

14 P. Tiwari, G. Agnihotri and A. K. Misra, *J. Carbohydr. Chem.*, 2005, **24**(7), 723–732.

15 R. Kakarla, R. G. Dulina, N. T. Hatzenbuhler, Y. W. Hui and M. J. Sofia, *J. Org. Chem.*, 1996, **61**(23), 8347–8349.

16 (*a*) H. Ohrui, H. Horiki, H. Kishi and H. Meguro, H., *Agric. Biol. Chem.*, 1983, **47**(5), 1101–1106; (*b*) Y. Nishida, H. Ohrui and H. Meguro, *Tetrahedron Lett.*, 1984, **25**(15), 1575–1578; (*c*) Y. Nishida, H. Hori, H. Ohrui and H. Meguro, *J. Carbohydr. Chem.*, 1988, **7**(1), 239–250.

17 H. Amarasekara, S. Dharuman, T. Kato and D. Crich, *J. Org. Chem.*, 2018, **83**(2), 881–897.

18 Linear regression equations: $P_{gg}=-23.8v+76.9$ ($R^2=0.92$); $P_{gt}=23.5v+22.1$ ($R^2=0.62$).

This journal is © The Royal Society of Chemistry 2025

Org. Biomol. Chem., 2025, **23**, 7000–7012 | **7011**

19 Linear regression equations: $P_{gg}=-25.6\nu+77.7$ (R^2=0.90); $P_{gt}=25.6\nu+22.1$ (R^2=0.87).

20 Linear regression equations: $P_{gg}=-18.1\nu+70.9$ (R^2=0.97); $P_{gt}=18.1\nu+29.1$ (R^2=0.97).

21 Linear regression equations: $P_{gg}=-17.5\nu+66.5$ (R^2=0.91); $P_{gt}=6.7\nu+39.3$ (R^2=0.21).

22 Linear regression equations: $P_{gg}=-13.8\nu+61.2$ (R^2=0.85); $P_{gt}=13.4\nu+32.6$ (R^2=0.53).

23 Linear regression equations: $P_{gg}=-13.1\nu+62.7$ (R^2=0.81); $P_{gt}=24.4\nu+22.4$ (R^2=0.97).

24 M. Charton, *J. Am. Chem. Soc.*, 1975, **97**(6), 1552–1556.

25 (*a*) R. W. Jr. Taft, *J. Am. Chem. Soc.*, 1952, **74**(11), 2729–2732; (*b*) R. W. Jr. Taft, *J. Am. Chem. Soc.*, 1952, **74**(12), 3120–3128; (*c*) R. W. Jr Taft, *J. Am. Chem. Soc.*, 1953, **75**(18), 4538–4539; (*d*) C. Hansch, A. Leo and R. W. Taft, *Chem. Rev.*, 1991, **91**(2), 165–195.

26 The Charton values used in this work are: methyl ν=0.52, ethyl ν=0.56, *n*-propyl ν=0.68, iso-propyl ν=0.79, cyclohexyl ν=0.87, and *tert*-butyl ν=1.24.

27 (*a*) N. Harada and K. Nakanishi, *Circular Dichroic Spectroscopy. Exciton Coupling in Organic Stereochemistry*, University Science Books, California, 1983; (*b*) *Circular Dichroism: Principles and Applications*, ed. N. Berova, K.

Nakanishi and R. W. Woody, Wiley-VCH, New York, N. Y., 2nd edn, 2000; (*c*) N. Harada, K. Nakanishi and N. Berova, *Electronic CD Exciton Chirality Method: Principles and Applications in Comprehensive Chiroptical Spectroscopy: Applications in Stereochemical Analysis of Synthetic Compounds, Natural Products, and Biomolecules*, ed. N. Berova, P. L. Polavarapu, K. Nakanishi and R. W. Woody, John Wiley & Sons, New York, NY, USA, 2012.

28 *Circular Dichroism and the Conformational Analysis of Biomolecules*, ed. G. D. Fasman, Plenum Press, New York, 1996, p. 25–157.

29 (*a*) A. E. Reed and P. von Ragué, *J. Am. Chem. Soc.*, 1990, **112**, 1434; (*b*) C. H. Patterson and R. P. Messmer, *J. Am. Chem. Soc.*, 1990, **112**, 4138; (*c*) R. P. Messmer, *J. Am. Chem. Soc.*, 1991, **113**, 433–440; (*d*) D. B. Chesnut and L. D. Quin, *J. Comput. Chem.*, 2004, **25**, 734–738; (*e*) F. A. M. Rudolph, A. L. Fuller, A. M. Z. Slawin, M. B. Bühl, R. A. Aitken and J. D. Woollins, *J. Chem. Crystallogr.*, 2010, **40**, 253–265.

30 (*a*) T. D. W. Claridge, *High-Resolution NMR Techniques in Organic Chemistry*, Elsevier Science, 3rd edn, 2016. DOI: **10.1016/C2015-0-04654-8**; (*b*) T. R. Hoye, P. R. Hanson and J. R. Vyvyan, *J. Org. Chem.*, 1994, **59**, 4096–4103.

7012 | *Org. Biomol. Chem.*, 2025, **23**, 7000–7012

This journal is © The Royal Society of Chemistry 2025